Transcriptome analysis of anaerobic glycolysis effects on Jurkat T cell proliferation

ZIYU WANG, HONGYANG WANG, QINGHAI WANG, TAO HUANG, CHEN GUO, JIANLEI JI, MEIJIE SU, WEIJIA XU, YANWEI CAO, ZHEN DONG

The Affiliated Hospital of Qingdao University, China

Abstract

Introduction: To explore the effects of anaerobic glycolysis on Jurkat T cell proliferation and clarify the possible mechanism via transcriptomic analysis.

Material and methods: The monocarboxylate transporter 1 inhibitor AZD3965 was used to target and block the transmembrane transport of lactate, thereby inhibiting anaerobic glycolysis in Jurkat T cells. Then, genes with differential expression between treated and untreated cells were detected by transcriptomic analysis, and constructs were generated. Gene Ontology (GO) and Kyoto Encyclopedia of Genes and Genomes (KEGG) pathway analyses as well as protein–protein interaction (PPI) network analysis were performed to explore the potential mechanism.

Results: Inhibition of anaerobic glycolysis reduced Jurkat T-cell proliferation. RNA sequencing identified 1723 transcripts that were differentially expressed, including 1460 upregulated genes and 263 downregulated genes. GO functional enrichment analysis showed that the differentially expressed genes were mainly involved in the biological processes of response to unfolded protein, response to topologically incorrect protein, and protein folding. KEGG pathway analysis of differentially expressed genes or hub genes from the PPI network analysis revealed enrichment in the estrogen signaling and PI3K-Akt pathways.

Conclusions: Anaerobic glycolysis contributes to the regulation of Jurkat T-cell proliferation. The underlying mechanism may involve the estrogen signaling pathway or PI3K-Akt signaling pathway as well as protein metabolism.

Key words: Jurkat T cell, anaerobic glycolysis, RNA sequencing, PI3K-Akt signaling pathway, HSP family.

Introduction

T lymphocytes, or T cells, act a central regulator of the immune response and play a vital role in the regulation of inflammation [1]. Specific roles of T cells have been detected in various disease states, such as chronic inflammation, tumors, and autoimmune diseases, and several types of T cells have been characterized, including cytotoxic T (Tc) cells, helper T (Th) cells, regulatory T cell (Tregs), γδ T cells, and natural killer (NK) T cells [2]. Although these cell types together account for only a small fraction (10-20%) of immune cells under physiological conditions, they play essential roles in the maintenance of immune homeostasis and are involved in the pathogenesis of various diseases [3]. For example, Tregs regulate immune homeostasis by suppressing the immune response and inducing peripheral tolerance [4].

Cell metabolism is a dynamic process that changes depending on the current bio-energetic requirement of cells [5]. The metabolic, energetic, and biosynthetic re-quirements of immune cells increase dramatically upon activation of these cells by antigens and mitogens. Establishment of a functional immune response requires rapid and extensive cell growth, proliferation, activation, and production of effector proteins [6]. Studies over the past several decades have revealed that T cells utilize diverse metabolic pathways for energy, molecular biosynthesis, and regulation of their proliferation, activation, differentiation and effector functions [7]. For example, effector T cells become exhausted and promote tumor cell evasion of immunosurveillance [8]. On the other hand, inhibition of glycolysis and glutaminolysis promotes differentiation of Th1 cells into Tregs [8]. Furthermore, Th17 cells are dependent on glycolysis mediated by hypoxia-inducible factor 1α (HIF-1α), and ablation of the HIF-1α pathway reduces the numbers of Th17 cells while increasing the Treg population [9]. Vitamin C reduces apoptosis and promotes proliferation of γδ T cells *via* increased oxidative respiration and glycolysis, which can enhance γδ T-cell expansion for adoptive immunotherapy [10].

T-cell activation alters cellular metabolism. The transition of T cells from a resting to an active state is accompanied by metabolic changes to meet the increased demands for energy and macromolecular synthesis for cell proliferation and effector functions. Metabolic alterations in activated T cells include increased glucose and glutamine consumption. Glucose and glutamine are metabolized by glycolysis and glutamine catabolism, respectively, to provide metabolic intermediates such as lactate and glutamate [11-13]. T-cell proliferation and activation are closely related to and regulated by metabolism. Therefore, it is necessary to investigate the metabolic fates of T cells and the corresponding impacts on their biological functions in different disease models, to gain insights for the development of novel strategies to restore the functionality of T cells.

T cells undergo metabolic reprogramming to continually satisfy their dynamic energetic and biosynthetic demands throughout their lifespan [14]. Circulating T cells are exposed to hypoxia in healthy and pathophysiological conditions, which may impact their biological activities [15]. Previous research showed that hypoxia reduces the infiltration and activity of CD8 T cells while increasing the activities of Tregs [16]. These effects were positively linked with metabolic changes and reflected metabolic reprogramming in T cells [17, 18]. Therefore, it is necessary to understand the effects of hypoxia on the biological functions of T cells, as this knowledge could enable the development of a targeted strategy for immune therapy for tumors. In the present study, we investigated the influence of anaerobic glycolysis on the proliferation of Jurkat T cells using RNA sequencing to identify proteins and signaling pathways involved in the molecular mechanism by which hypoxia induces metabolism changes in Jurkat T cells. The results of this study may provide insight into the molecular mechanism of tumor immune escape, and thereby support the development of novel strategies for tumor immunotherapy.

Material and methods

Cell culture

This study was approved by the Ethics Committee of Qingdao University Hospital. The Jurkat T cell line Clone E6-1 was purchased from Wuhan Procell Life Science & Technology Co, Ltd. RPMI-1640 medium supplemented with 10% fetal bovine serum (FBS; Gibco, USA) was used for cell culture. Cells were cultured in a 5% CO_2 atmosphere at 37°C and trypsinized and passaged at a 1 : 3 ratio once they had reached 80% confluence.

Lactate dehydrogenase activity

To measure lactate dehydrogenase (LDH) production by T cells, aliquots of 1×10^5 cells were seeded in 96-well plates and exposed to either dimethyl sulfoxide (DMSO, 0.01%) or different concentrations of the monocarboxylate transporter 1 (MCT1) inhibitor AZD3965 (0, 5, 10, 50, 100, and 500 nM, MedChemExpress, China) to block transmembrane transport of lactate, thereby inhibiting anaerobic glycolysis. After 24 h of treatment, the culture medium was collected and incubated with Lactate Dehydrogenase Activity Assay Kit (Sigma, America) at 37°C for 10 min. The amount of LDH was measured by detection of absorbance at 490 nm with a reference wavelength of 655 nm using a spectrophotometer (Sysmex cube6, Japan).

Cell proliferation cell counting kit-8

Cell proliferation was assessed by cell counting kit-8 (CCK-8) evaluation. Briefly, 1×10^5 Jurkat cells were seeded in 96-well plates and exposed to either DMSO (0.01%) or different concentrations of AZD3965 (0, 5, 10, 50, 100, and 500 nM) for 24 h. The numbers of cells in the wells were detected using the CCK-8 (Dojindo, Tokyo, Japan). Optical density (OD) values at 450 nm were detected using a Multiskan Go spectrophotometer (Thermo Fisher Scientific, USA).

RNA sequencing

For RNA-sequencing analysis, Jurkat Clone E6-1 cells were seeded and exposed to either DMSO or AZD3965 (100 nM) for 24 h. Total RNA was extracted using the Trizol reagent kit (Invitrogen, Carlsbad, CA, USA) according to the manufacturer's protocol. RNA quality was assessed on an Agilent 2100 Bioanalyzer (Agilent Technologies, Palo Alto, CA, USA) and checked using RNase free agarose gel electrophoresis. Extracted total RNA was treated with Oligo(dT) beads to enrich eukaryotic mRNA. The enriched mRNA was fragmented into short fragments using fragmentation buffer and reverse transcribed into cDNA using the NEBNext Ultra RNA Library Prep Kit for Illumina (NEB #7530, New England Biolabs, Ipswich, MA, USA).

The purified double-stranded cDNA fragments were end repaired, subjected to the addition of an A base, and ligated to Illumina sequencing adapters. The ligation reaction was purified with the AMPure XP Beads (1.0×). Ligated fragments were subjected to size selection by agarose gel electrophoresis and polymerase chain reaction (PCR) amplified. The resulting cDNA library was sequenced using Illumina Novaseq6000 by Gene Denovo Biotechnology Co. (Guangzhou, China).

All high-throughput sequencing image data were converted into sequence data (Reads) by CASAVA base recognition. Reads that were adapter-polluted or of low quality and those in which the number of N bases accounted for > 5% were removed. The data were filtered using Trim-galore software to remove adapters from the sequence. After filtering, the proportion of the sequence that remained for each sample after the quality control step was examined, and the proportion of the sequence that was filtered was plotted. At the same time, a cumulative histogram of the filtering sequence was prepared.

The QPhred score was used to measure the sequencing quality. Sequences were judged as having sufficient quality if the average Q20 was ≥ 85% and the average Q30 was ≥ 80%. A histogram of the mean base error rate was generated to reflect the quality of single bases in a sequence. An index of the reference genome was built, and paired-end clean reads were mapped to the reference genome using HISAT2. 2.4 with "-rna-strandness RF" and other parameters set as a default. After the alignment, the aligned genome sequences were assembled and gffcompare software was used to compare the aligned genome sequences with the original genome annotation information to identify new transcripts or new genes of the species. The gffcompare software could classify the transcripts according to the comparison results with the reference transcriptome.

After a series of normalization steps, gene expression levels were measured and quantitatively analyzed by StringTie software. The results are represented in boxplot form. Fragment counts for each gene in each sample were provided by StringTie (Version 2.2.0). For each transcription region, an FPKM (fragments per kilobase of transcript per million mapped reads) value was calculated to quantify its expression abundance and variations, using RSEM software. The calculated gene expression values can be directly used to detect differences in gene expression among samples. The gene expression values were analyzed by principal component analysis (PCA), and the PCA map was drawn. Differential RNA expression analysis was performed using DESeq2 software for comparisons between two different groups (and by edgeR for comparisons between two samples). The genes/transcripts with a false discovery rate (FDR) < 0.05 and an absolute fold change ≥ 1 were considered differentially expressed genes/transcripts.

Bioinformatic analysis

Functional enrichment analysis of the differentially expressed RNAs was performed using David (https://david.ncifcrf.gov/). The statistical significance of each enrichment was assessed by the corrected p-value (Benjamini–Hochberg method). For Gene Ontology (GO) functional enrichment, p-adj < 0.05 was used as the threshold for significant enrichment. From the GO enrichment analysis results, the most significant GO entries in the three components of CC (Cellular Component), BP (Biological Process), and MF (Molecular Function) were selected and combined for preparation of a bar graph and dot graph. For the Kyoto Encyclopedia of Genes and Genomes (KEGG) functional enrichment analysis, p-adj < 0.05 was applied as the threshold for significant enrichment. The signaling pathways were illustrated in histograms and dot plots.

Protein–protein interaction network analysis

String (https://www.string-db.org/) was used to assess the protein–protein interaction (PPI) network. The inter-action relationships in the STRING protein interaction database were used to analyze the differential gene–protein interaction network. All significantly differentially expressed genes in each group were mapped to the STRING database, and the PPI network information was extracted, including the names of the interacting proteins and information on the confidence and strength of the binding between pairs. The PPI was constructed from the differentially expressed genes, and the MCODE plug-in of Cytoscape software was used to identify the key nodes in the network. Then the hub genes were imported into Metascape, and the GO and KEGG databases were used for pathway analysis. A confidence score > 0.7 was considered statistically significant.

Statistical analysis

Each experiment was repeated at least three times. All statistical analyses were conducted using R (version 3.6.3). Data are expressed as mean ± standard deviation values. Significant differences between two groups were identified by Student's t-test, with $p < 0.05$ indicating statistical significance.

Results

Inhibition of anaerobic glycolysis repressed Jurkat T cell proliferation

To detect the influence of anaerobic glycolysis on the proliferation of Jurkat T cells, AZD3965 was used to inhibit anaerobic glycolysis. The results showed that AZD3965 treatment decreased the generation of LDH in a dose-dependent manner in the dose range 0-100 nM (Fig. 1A). However, with the higher concentration of 500 nM, no significant further decrease in LDH generation was observed, and cell viability was obviously attenuated. CCK-8 analysis also showed that AZD3965 treatment decreased the rate of cell proliferation in a dose-dependent manner in the dose range 0-100 nM (Fig. 1B). These results indicated that inhibition of anaerobic glycolysis attenuated the proliferation of Jurkat T cells.

Inhibition of anaerobic glycolysis altered the expression profile in Jurkat T cells

To gain insight into the molecular mechanism underlying the influence of anaerobic glycolysis on Jurkat T-cell proliferation, we conducted transcriptomic sequencing for Jurkat cells treated with or without AZD3965. This analysis identified 1723 genes that were differently expressed with inhibition of anaerobic glycolysis by treatment with AZD3965 (Fig. 2A). Of these, 1460 genes were upregulated, including *BBC3*, *SLC6A9*, *INHBC*, *BEST1*, and *HOXB9*, and 263 genes were downregulated, including *UTP14C*, *SNORA26*, *LNX1*, and *ZNF793* (Fig. 2B).
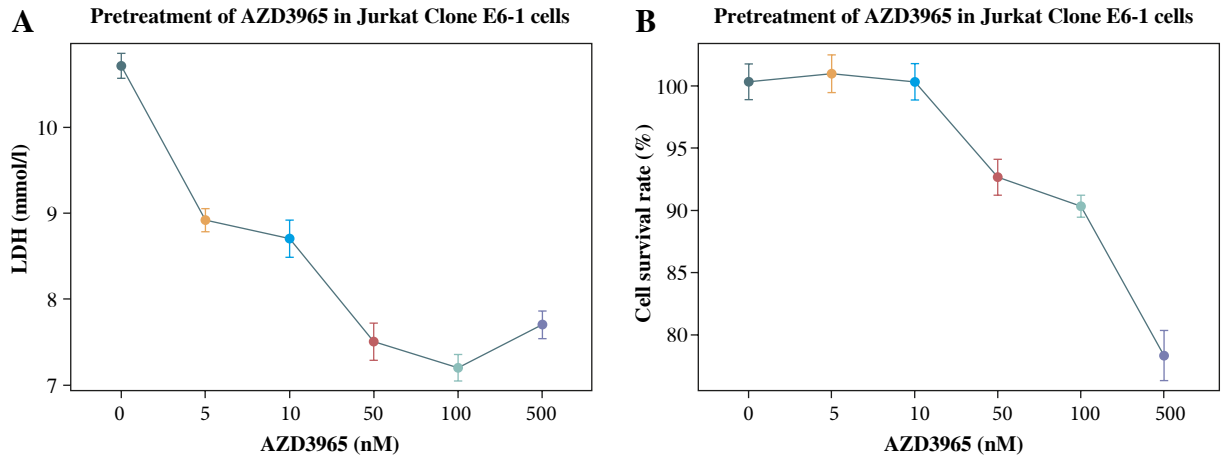
Fig. 1. A) Concentration of lactate dehydrogenase (LDH) in medium from Jurkat T cells treated with different concentrations of AZD3965. **B**) Viability of Jurkat T cells treated with different concentrations of AZD3965. Data were from three independent experiments
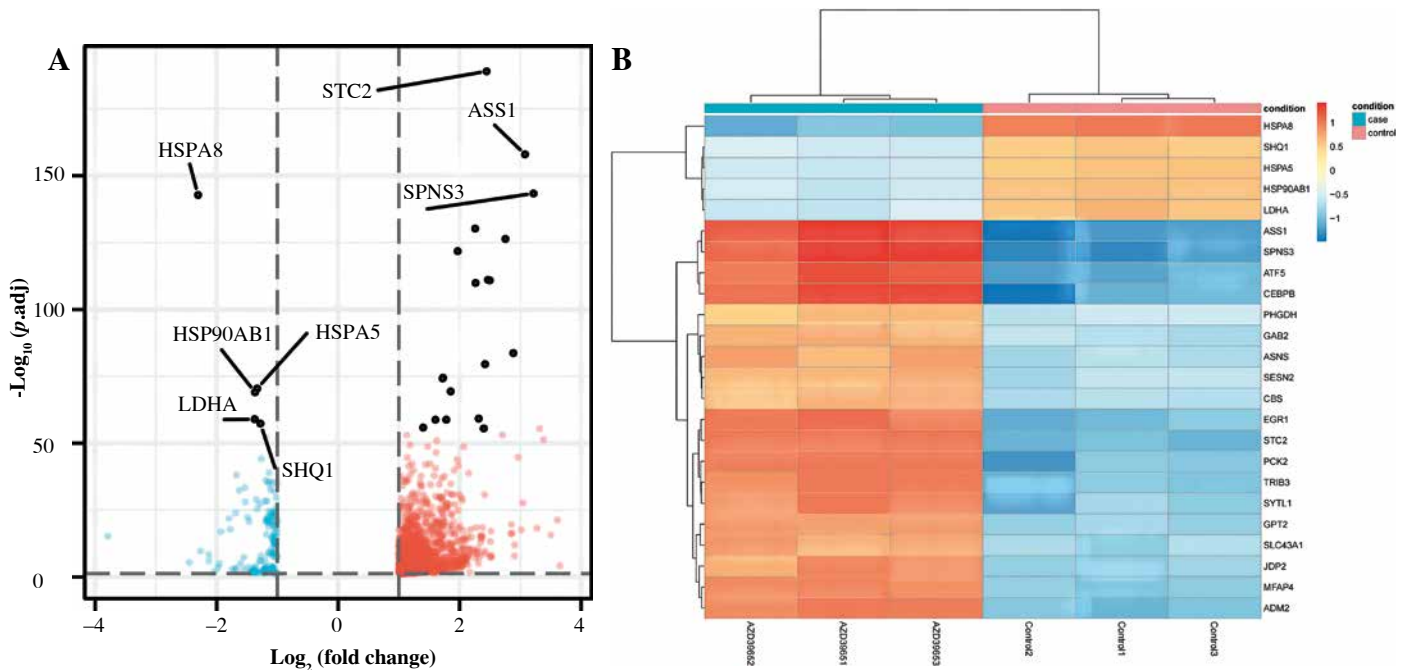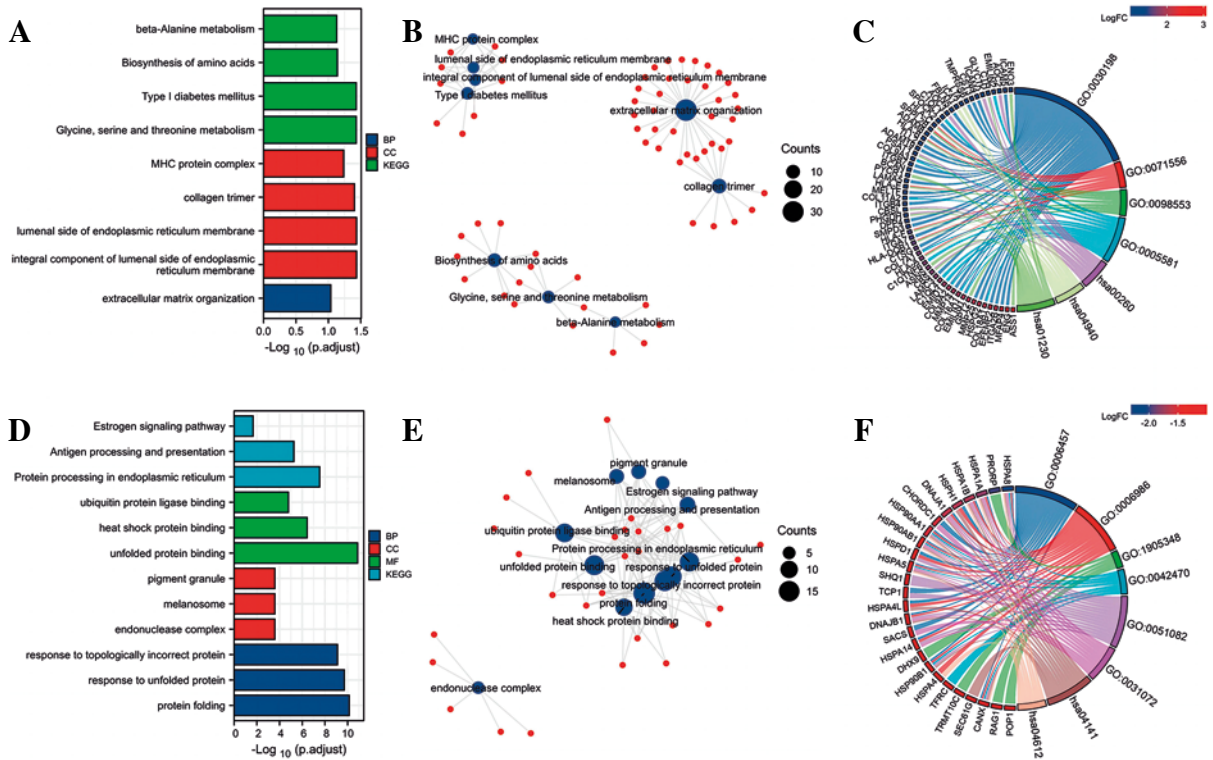

Fig. 2. Differentially expressed genes in Jurkat T cells treated with or without AZD3965. **A**) Volcano plot of differentially expressed genes. **B**) Heat map of differentially expressed genes

Notably, genes of the heat shock protein (HSP) family, including *HSPA8*, *HSPA5*, *HSPA1A*, and *HSPA1B*, were also significantly downregulated (Fig. 2B).

Expression of genes regulating cell proliferation was dysregulated upon inhibition of anaerobic glycolysis

To further analyze the functional importance of the differentially expressed genes, we performed GO enrichment

and KEGG pathway analyses (Fig. 3A, B). For the upregulated genes, the result of GO analysis showed enrichment for genes involved in extracellular matrix organization. These genes included members of the integrin family (*ITGA2B*, *ITGA7*, *ITGB4*, and *ITGB7*), collagen family (*COL7A1*, *COL9A2*, *COL9A3*, *COL11A2*, *COL16A1* and others), and human leukocyte antigen (HLA) family (*HLA-A*, *HLA-B*, *HLA-C*, *HLA-DQB1*, *HLA-E*, *HLA-F*, *SPPL2B* and others) (Fig. 3C). Other genes were involved in the integral component of the endoplasmic reticulum

Fig. 3. Gene Ontology (GO) and Kyoto Encyclopedia of Genes and Genomes (KEGG) analysis of differentially expressed genes. **A**) Significantly enriched GO biological processes for the upregulated genes. **B**) Upregulated genes that contributed to GO and KEGG clusters. **C**) Chord diagram showing enriched GO and KEGG clusters for the upregulated genes implicated in the regulation of Jurkat T-cell proliferation. In each chord diagram, enriched GO and KEGG clusters are shown on the right, and genes contributing to this enrichment are shown on the left. **D**) Significantly enriched GO biological processes for the downregulated genes. **E**) Downregulated genes that contributed to the GO and KEGG clusters. **F**) Chord diagram showing enriched GO and KEGG clusters for the downregulated genes implicated in the regulation of Jurkat T-cell proliferation. In each chord diagram, enriched GO and KEGG clusters are shown on the right, and genes contributing to this enrichment are shown on the left

lumen, collagen trimer, and major histocompatibility complex (MHC) protein complex (Fig. 3A, B). Notably, upregulated genes including integrin family members, *DPP4*, and *SMPD3* served as inhibitors of cell proliferation. KEGG pathway enrichment analysis also revealed that the differentially expressed genes were mainly enriched in glycine, serine and threonine metabolism, type I diabetes mellitus, biosynthesis of amino acids, and beta-alanine metabolism (Fig. 3A, B). For the downregulated genes, GO analysis showed enrichment for genes involved in the response to unfolded protein, response to topologically incorrect protein, protein folding, and response to heat (Fig. 3D, E). KEGG pathway enrichment analysis also revealed that the differentially expressed genes were mainly enriched in protein processing in endoplasmic reticulum, antigen processing and presentation, the estrogen signaling pathway, and legionellosis (Fig. 3D, E). Notably, HSP family proteins (HSPA1A, HSPA1B, HSPA8, HSP90AA1, HSP90AB1, HSP90B1 etc.), which can promote cell proliferation, were significantly involved in these processes

(Fig. 3F). These results indicate that inhibition of anaerobic glycolysis could impact protein metabolism, extracellular matrix organization, and the expression of genes involved in cell proliferation. Moreover, the estrogen signaling pathway was found to be potentially involved in this process.

PPI network analysis revealed additional functions of dysregulated genes

To further analyze the functions of differentially expressed genes, PPI network analysis was performed. As shown in Figure 4A, many hub genes, including HSP family protein genes, ERBB2, UBC, DNAJB1, and NME1-NME2, were identified. To further clarify the functions of these hub genes, GO and KEGG pathway analyses of these genes were performed. The results also showed they were mainly involved in the response to unfolded protein, response to topologically incorrect protein, and protein folding (Fig. 4B). KEGG pathway enrichment analysis also revealed that these hub genes were mainly enriched in
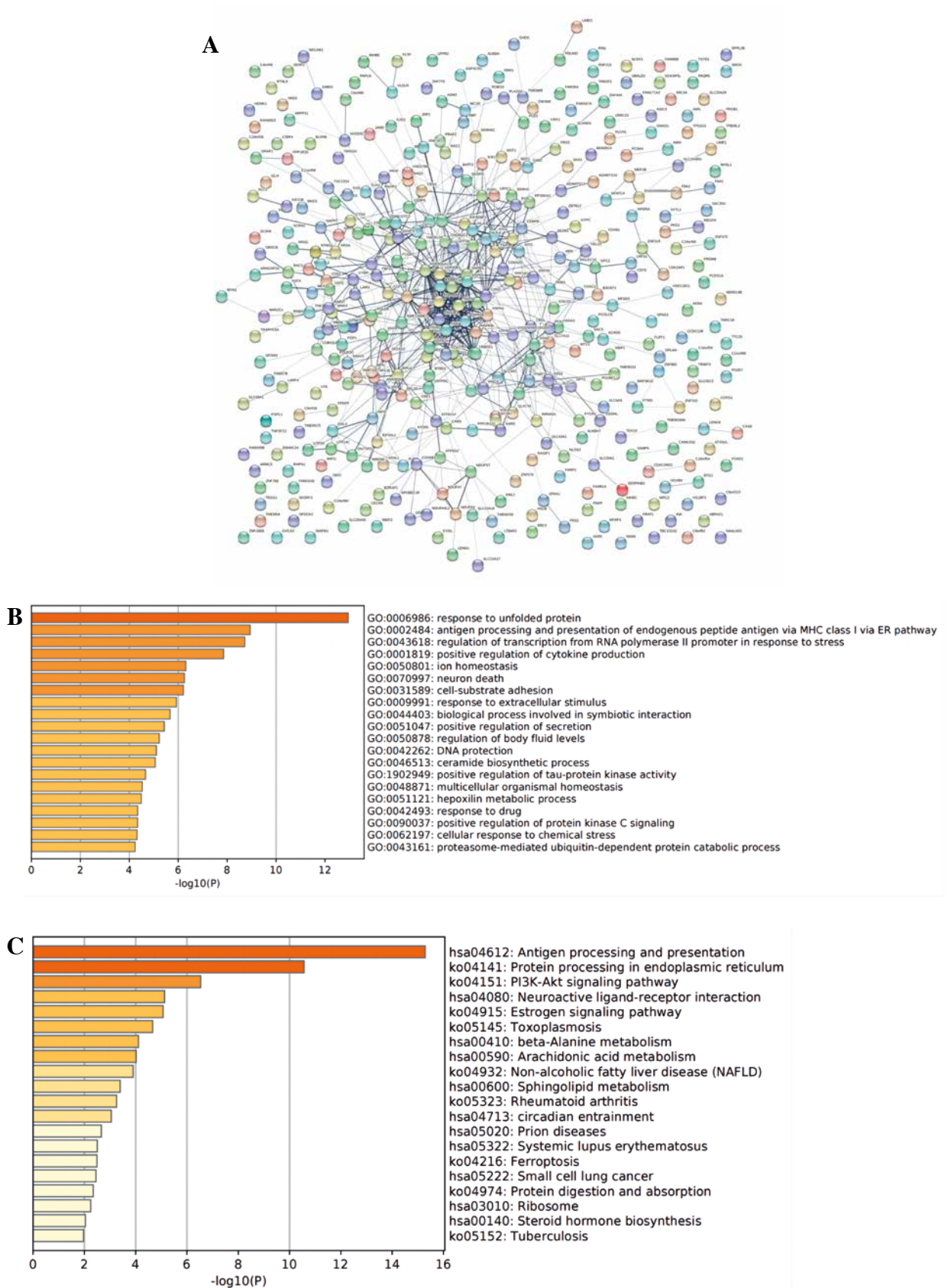
Fig. 4. A) Protein–protein interaction (PPI) network. Results of **B**) Gene Ontology (GO) and **C**) Kyoto Encyclopedia of Genes and Genomes (KEGG) analyses of PPI hub genes

antigen processing and presentation, protein processing in endoplasmic reticulum, the PI3K-Akt signaling pathway, neuroactive ligand–receptor interaction, and the estrogen signaling pathway (Fig. 4C).

Discussion

Glycolysis is an essential process for cell activation as it can generate energy for proliferation [19], and the metabolic processes of T cells change under different conditions [20]. Inhibition of anaerobic glycolysis in T cells is known to induce a chronic negative energy balance, and previous research showed that inhibition of anaerobic glycolysis can alter T-cell transcription related to immune responses [21]. In the present study, inhibition of anaerobic glycolysis significantly altered the expression profile in Jurkat cells. We found that the differentially expressed genes were mainly enriched in extracellular structure organization: antigen processing and presentation; glycine, serine and threonine metabolism; and type I diabetes mellitus pathways.

In this study, the MCT1 inhibitor AZD3965 was used to inhibit anaerobic glycolysis in Jurkat T cells. MCTs are proton-linked transmembrane proteins belonging to the solute carrier 16A family and are involved in the influx–efflux mechanisms of monocarboxylates such as lactate and pyruvate [22]. MCT1 optimally imports lactate, and its activity has been linked to cancer aggressiveness and poor outcomes [23]. Cancer cells rely on glycolysis for survival and rapid proliferation in a hypoxic tumor microenvironment [24]. MCT1 is generally overexpressed in different types of cancer cells due to hypoxia [22]. AZD3965, alone or combined with other interventions, successfully decreased tumor growth and promoted intracellular lactate accumulation in animal models [23]. The Phase I study of AZD3965 showed that it was tolerated and demonstrated preliminary antitumor activity in advanced cancers [25].

Intracellular oxygen metabolism is an important factor affecting tumor immunosuppression [26]. The functional activity of T cells is also affected by the local tissue microenvironment, especially changes in oxygen concentration [27]. Many studies have confirmed that the local microenvironment of tumors is hypoxic, as observed in cervical and head and neck squamous cell carcinoma [28]. This hypoxic state can inhibit the activation and proliferation of T cells and affect their differentiation into Th1 cells [29]. For example, the hypoxia-activated apoptosis signaling pathway is activated in γδ T cells, thereby inhibiting the anti-tumor function of γδ T cells [30]. Previous research also demonstrated that hypoxia promotes T-cell apoptosis by downregulation of CCR7 [31]. In the present study, we noted that anaerobic glycolysis specifically affected the expression of HSP family genes (*HSPA8, HSPA5, HSP-90AB1*, etc.) as well as the *LDHA* gene and *SHQ1* gene. HSP expression increases when the body is stimulated by hypoxia, and increased expression of these proteins has

anti-apoptotic effects [32]. In fact, most HSP genes are targets of HIF-1 [33]. For example, HIF-1 can induce the transcription of Hsp70 under hypoxic conditions [34]. Mechanistically, HSPs can promote cell proliferation through regulation of cell cycle progression by stabilization of cyclinD1-CDK4/6 and cyclinE1-CDK2 [35]. Inhibition of anaerobic glycolysis downregulated the expression of HSPs, which might impact cell cycle progression and decrease the cell proliferation rate. Relevant studies have shown that inhibition of LDHA can activate GCN2-ATF4 signal transduction, reduce the synthesis of intracellular serine and aspartate, and inhibit cell proliferation [36]. Furthermore, SHQ1 is essential to the processing of ribosomal RNAs, the modification of spliceosome small RNAs, and the stabilization of telomerase [37]. Thus, decreased expression of SHQ1 will affect cell proliferation by inhibiting transcription.

The additional genes *STC2*, *SPNS3*, and *ASS1* were significantly upregulated when anaerobic glycolysis was inhibited in Jurkat T cells. STC2 is a disulfide-bonded homodimer secreted glycoprotein that plays a role in various physiological processes such as cellular metabolism, inflammation, endoplasmic reticulum and oxidative stress, calcium regulation, cell proliferation, and apoptosis [38]. STC2 was previously shown to be overexpressed under hypoxia and stress conditions, and to contribute to cell protection and apoptosis inhibition [39]. ASS1 is a urea cycle enzyme that is essential for the conversion of nitrogen from ammonia and aspartate to urea. Previous research showed that overexpression of ASS1 reduces intracellular aspartate levels by downregulating its substrate utilization and lactation [40]. The mammalian target of rapamycin (mTOR) pathway inhibits S6K1 phosphorylation to inhibit activation of CAD (carbamoyl phosphate synthetase 2, aspartate aminotransferase and dihydrogenase complex), thereby reducing pyrimidine synthesis to inhibit cell proliferation. SPNS3 protein is involved in the cell membrane transport of sphingolipids, and its expression level may have predictive significance for the prognosis of acute myeloid leukemia [41]. These dysregulated genes might contribute to the regulation of Jurkat T cell proliferation.

KEGG pathway analysis showed that the differentially expressed genes were enriched in the estrogen signaling pathway. However, after PPI network analysis, KEGG pathway analysis showed that the hub genes were enriched in the PI3K-Akt signaling pathway, which is involved in cell proliferation and apoptosis [42]. Notably, genes involved in this pathway including HSP family members (*HSP90AA1, HSP90AB1*, and *HSP90B1*) and *CDH2* were significantly down-regulated. Inhibition of the PI3K-Akt signaling pathway impairs activation of the mTOR pathway, which reduces the synthesis of downstream molecules including S6K, 4EBP1 and p34, ultimately inhibiting cell proliferation [43, 44]. Recently, increasing attention has been paid to the impact of the estrogen signaling path-

way on T cell proliferation and differentiation [45]. In this study, we also noted that the estrogen signaling pathway was affected by inhibition of anaerobic glycolysis in Jurkat T cells. Previous research showed that proliferation of T cells was significantly affected in mice lacking estrogen receptor alpha (Erα), and Foxp3 expression was increased [46]. Therefore, inhibition of anaerobic glycolysis may inhibit the proliferation of Jurkat T cells through alteration of PI3K-Akt signaling and estrogen signaling.

There are some limitations of this study. The leukemic Jurkat cell line, rather than primary T cells, was used, which may affect the generalization of our results. The Jurkat T cell line is the best-known T-cell model for studying the signaling machinery engaged by T-cell receptors [47]. Moreover, previous research has confirmed that MCT-1 inhibition can also inhibit the proliferation of primary T cells [48]. However, MCT-1 inhibition did not affect processes related to lymphocyte activation, such as cytokine production [48]. Therefore, further studies using primary T cells are needed to investigate the effects of anaerobic glycolysis on lymphocyte activation, which may also be involved in tumor progression.

Conclusions

The present study demonstrated that anaerobic glycolysis contributes to the regulation of Jurkat T cell proliferation and inhibition of anaerobic glycolysis decreases the proliferation of Jurkat T cells. The underlying mechanism may involve dysregulated expression of genes encoding the HSP family members and proteins involved in the PI3K-Akt signaling pathway and estrogen signaling pathway.

Funding

Disclosures

Approval of the Bioethics Committee was not required. The authors declare no conflict of interest.

References

1. Coulie P, Van den Eynde B, van der Bruggen P, Boon T (2014): Tumour antigens recognized by T lymphocytes: at the core of cancer immunotherapy. Nat Rev Cancer 14: 135-146.
2. Velardi E, Tsai J, van den Brink M (2021): T cell regeneration after immunological injury. Nat Rev Immunol 21: 277-291.
3. Gaud G, Lesourne R, Love P (2018): Regulatory mechanisms in T cell receptor signalling. Nat Rev Immunol 18: 485-497.
4. Hosokawa H, Rothenberg E (2021): How transcription factors drive choice of the T cell fate. Nat Rev Immunol 21: 162-176.
5. von Meyenn L, Bertschi N, Schlapbach C (2019): Targeting T cell metabolism in inflammatory skin disease. Front Immunol 10: 2285.
6. Mateo J, García-Lecea M, Cadenas S, et al. (2003): Regulation of hypoxia-inducible factor-1alpha by nitric oxide through mitochondria-dependent and -independent pathways. Biochem J 376: 537-544.
7. Hu C, Xuan Y, Zhang X, et al. (2022): Immune cell metabolism and metabolic reprogramming. Mol Biol Rep 49: 9783-9795.
8. Chakraborty S, Khamaru P, Bhattacharyya A (2022): Regulation of immune cell metabolism in health and disease: special focus on T and B cell subsets. Cell Biol Int 46: 1729-1746.
9. Huang J, Li Z, Hu Y, et al. (2022): Melatonin, an endogenous hormone, modulates Th17 cells via the reactive-oxygen species/TXNIP/HIF-1α axis to alleviate autoimmune uveitis. J Neuroinflammation 19: 124.
10. Kouakanou L, Xu Y, Peters C, et al. (2020): Vitamin C promotes the proliferation and effector functions of human γδ T cells. Cell Mol Immunol 17: 462-473.
11. Johnson MO, Siska PJ, Contreras DC, Rathmell JC (2016): Nutrients and the microenvironment to feed a T cell army. Semin Immunol 28: 505-513.
12. Maciolek JA, Pasternak JA, Wilson HL (2014): Metabolism of activated T lymphocytes. Curr Opin Immunol 27: 60-74.
13. Buck MD, O'Sullivan D, Pearce EL (2015): T cell metabolism drives immunity. J Exp Med 212: 1345-1360.
14. Jiao B, Liu S, Zhao H, et al. (2022): Hypoxia-responsive circRNAs: A novel but important participant in non-coding RNAs ushered toward tumor hypoxia. Cell Death Dis 13: 666.
15. Mortezaee K, Majidpoor J (2021): The impact of hypoxia on immune state in cancer. Life Sci 286: 120057.
16. Hu J, Li X, Yang L, Li H (2022): Hypoxia, a key factor in the immune microenvironment. Biomed Pharmacother 151: 113068.
17. Xu L, Ma Q, Zhu J, et al. (2018): Combined inhibition of JAK1,2/Stat3-PD-L1 signaling pathway suppresses the immune escape of castration-resistant prostate cancer to NK cells in hypoxia. Mol Med Rep 17: 8111-8120.
18. You L, Wu W, Wang X, et al. (2021): The role of hypoxia-inducible factor 1 in tumor immune evasion. Med Res Rev 41: 1622-1643.
19. Nguyen HD, Kuril S, Bastian D, Yu XZ (2018): T-cell metabolism in hematopoietic cell transplantation. Front Immunol 9: 176.
20. Sun L, Fu J, Zhou Y (2017): Metabolism controls the balance of Th17/T-regulatory cells. Front Immunol 8: 1632.
21. Jung J, Zeng H, Horng T (2019): Metabolism as a guiding force for immunity. Nat Cell Biol 21: 85-93.
22. Wang Y, Qin L, Chen W, et al. (2021): Novel strategies to improve tumour therapy by targeting the proteins MCT1, MCT4 and LAT1. Eur J Med Chem 226: 113806.
23. Silva A, Antunes B, Batista A, et al. (2021): In vivo anticancer activity of AZD3965: A systematic review. Molecules 27: 181.
24. Al Tameemi W, Dale TP, Al-Jumaily RMK, Forsyth NR (2019): Hypoxia-modified cancer cell metabolism. Front Cell Dev Biol 7: 4.
25. Halford S, Veal GJ, Wedge SR, et al. (2023): A phase I dose-escalation study of AZD3965, an oral monocarboxylate transporter 1 inhibitor, in patients with advanced cancer. Clin Cancer Res 29: 1429-1439.
26. Roy S, Rizvi Z, Awasthi A (2018): Metabolic checkpoints in differentiation of helper T cells in tissue inflammation. Front Immunol 9: 3036.
27. Bao M, Wong C (2021): Hypoxia, metabolic reprogramming, and drug resistance in liver cancer. Cells 10: 1715.

28. Chihanga T, Vicente-Muńoz S, Ruiz-Torres S, et al. (2022): Head and neck cancer susceptibility and metabolism in Fanconi anemia. Cancers 14: 2040.

29. Santos S, Lira F, Silva E, et al. (2019): Effect of moderate exercise under hypoxia on Th1/Th2 cytokine balance. Clin Respir J 13: 583-589.

30. Li Y, Wang Y, Shi F, et al. (2022): Phospholipid metabolites of the gut microbiota promote hypoxia-induced intestinal injury via CD1d-dependent γδ T cells. Gut Microbes 14: 2096994.

31. Liu J, Zhang X, Chen K, et al. (2019): CCR7 chemokine receptor-inducible lnc-Dpf3 restrains dendritic cell migration by inhibiting HIF-1α-mediated glycolysis. Immunity 50: 600-615.e615.

32. Moura C, Lollo P, Morato P, Amaya-Farfan J (2018): Dietary nutrients and bioactive substances modulate heat shock protein (HSP) expression: a review. Nutrients 10: 683.

33. Ban H, Han T, Hur K, Cho H (2019): Epigenetic alterations of heat shock proteins (HSPs) in cancer. Int J Mol Sci 20: 4758.

34. Agarwal S, Ganesh S (2020): Perinuclear mitochondrial clustering, increased ROS levels, and HIF1 are required for the activation of HSF1 by heat stress. J Cell Sci 133: jcs245589.

35. Ahn J, Zhou X, Dowd S, et al. (2013): Insight into hypoxia tolerance in cowpea bruchid: metabolic repression and heat shock protein regulation via hypoxia-inducible factor 1. PLoS One 8: e57267.

36. Pathria G, Scott DA, Feng Y, et al. (2018): Targeting the Warburg effect via LDHA inhibition engages ATF4 signaling for cancer cell survival. EMBO J 37: e99735.

37. Sleiman S, Marshall AE, Dong X, et al. (2022): Compound heterozygous variants in SHQ1 are associated with a spectrum of neurological features, including early-onset dystonia. Hum Mol Genet 31: 614-624.

38. Joshi A, Thinakaran G, Elferink C (2022): Cinnabarinic acid-induced stanniocalcin 2 confers cytoprotection against alcohol-induced liver injury. J Pharmacol Exp Ther 381: 1-11.

39. Li Q, Zhou X, Fang Z, Pan Z (2019): Effect of STC2 gene silencing on colorectal cancer cells. Mol Med Rep 20: 977-984.

40. Rabinovich S, Adler L, Yizhak K, et al. (2015): Diversion of aspartate in ASS1-deficient tumours fosters de novo pyrimidine synthesis. Nature 527: 379-383.

41. Somanath P, Chen J, Byzova T (2008): Akt1 is necessary for the vascular maturation and angiogenesis during cutaneous wound healing. Angiogenesis 11: 277-288.

42. Huang W, Qian T, Cheng Z, et al. (2020): Prognostic significance of Spinster homolog gene family in acute myeloid leukemia. J Cancer 11: 4581-4588.

43. Ersahin T, Tuncbag N, Cetin-Atalay R (2015): The PI3K/AKT/mTOR interactive pathway. Mol Biosyst 11: 1946-1954.

44. Xia P, Xu XY (2015): PI3K/Akt/mTOR signaling pathway in cancer stem cells: from basic research to clinical application. Am J Cancer Res 5: 1602-1609.

45. Vrtačnik P, Ostanek B, Mencej-Bedrač S, Marc J (2014): The many faces of estrogen signaling. Biochem Medica 24: 329-342.

46. Mohammad I, Starskaia I, Nagy T, et al. (2018): Estrogen receptor α contributes to T cell-mediated autoimmune inflammation by promoting T cell activation and proliferation. Sci Signal 11: eaap9415.

47. Abraham RT, Weiss A (2004): Jurkat T cells and development of the T-cell receptor signalling paradigm. Nat Rev Immunol 4: 301-308.

48. Murray CM, Hutchinson R, Bantick JR, et al. (2005): Monocarboxylate transporter MCT1 is a target for immunosuppression. Nat Chem Biol 1: 371-376.